

# Modeling of Unsteady Two-Phase Flow over a Stretching Sheet with Analysis of Heat and Mass Transfer due to Electrification of Particles and Viscous Dissipation

Aswin Kumar Rauta<sup>1</sup> and Saroj Kumar Mishra<sup>2</sup>

*1 Lecturer, Department of Mathematics, S.K.C.G.College, Paralakhemundi, Odisha,India*

*2 Professor, Centre for Fluid Dynamics Research,Department of Mathematics, Centurian University of Technology and Management , Paralakhemundi, Odisha, India*

*Email:aswinmath2003@gmail.com*

## Abstract:

This paper is intended to investigate the effect of electrification of particles, terms related to the heat added to the system to slip-energy flux and heat due to conduction and viscous dissipation in the energy equation of the particle phase in simulating the boundary layer flow and heat transfer in presence of heat generation/absorption, radiation and electrification of particles over a stretching sheet. The governing partial differential equations of the flow field are reduced into first order ordinary differential equations using similarity transformations and then solved numerically using Runge-Kutta method with shooting technique. Numerical results obtained to study the effects of various parameters like Prandtl Number, Eckert Number, Grashof Number, electrification parameter, radiation parameter, and heat source/sink parameter on dimensionless velocity, temperature as well as the skin friction and Nusselt number. Comparison of the obtained results is made with existing literature and graphical study is performed to explain the inter relationship between parameters and velocity, parameters and heat transfer. The rate of heat transfer at the surface and skin friction increases with increasing values of electrification parameter  $M$ . Thermal boundary layer thickness of fluid phase increases but thermal boundary layer thickness of dust phase decrease for the enhanced values of diffusion parameter  $\epsilon$ .

**Key words:** Boundary-Layer, Dusty fluid, Electrification of particles, Heat source / sink, Nusselt number, Radiation, Skin Friction Coefficient, Stretching Sheet, Two-phase flow ,Unsteady Flow.

## 1. Introduction:

The investigation of radiation, heat generation/absorption and electrification of particles are crucial because, their effects on the flow field and heat transfer analysis of unsteady two-phase flow over a stretching sheet have several applications like cooling of nuclear reactor, aerospace component production, petroleum industry, metal casting, physiological flows, food processing, lubrication, heat removal from nuclear fuel debris, the aerodynamic extrusion of plastic sheet, glass blowing, cooling or drying of papers, drawing plastic films, extrusion of polymer melt-spinning process, rolling and manufacturing of plastic films, purification of crude oil and artificial fibers cooling industry of dying etc. The importance of such flow problems involving high temperature regime lies in the fact that the mechanical properties of final product are influenced by stretching rate and the rate of cooling. The rate of stretching is important because the rapid stretching results in sudden solidification, thereby destroying the properties expected for outcomes. In fact the rate of heat transfer over a surface has a pivotal role in the quality of final products. So the radiate heat transfer cannot be ignored in the industrial process involving high temperature regime and good working knowledge of it helps designing pertinent equipments. Due to wide area of applications and simple geometry; many researchers have studied boundary layer flow and heat transfer over a stretched surface and have presented the numerical and analytical solutions for

various flow characteristics. These areas have potential applications in industries which have important contributions for the progress of the society.

Sakiadis B.C. [43] first explored the study of boundary layer flow over a continuous moving flat surface .He has used both exact and approximate method to investigate it. Sakiadis's theoretical predictions for Newtonian fluids were later verified experimentally by Tsou et al. [51] and extended the same work to the heat transfer case. Crane L.J. [10] extended this problem to a stretching sheet whose surface velocity varies linearly with the distance  $x$  from a fixed origin and obtained the similarity solution. Since then, research area of stretching sheet has been flooded with many research articles with multiple dimensions enriched by the innovative researchers. An exact similarity solution for the dimensionless differential system was obtained. Then such closed form similarity solution has been obtained for several other features like viscoelastic magnetohydrodynamics (MHD), suction, porosity and heat source/sink. Grubka L.J.et.al. [19] discussed the temperature field in the flow over a stretching surface when a uniform heat flux is exerted to the surface. Recently, a new idea is added to the study of boundary layer fluid flow and heat transfer. Indeed, in such studies, the effects of thermal radiation and temperature dependent viscosity are included. Rashidi et.al.[41] have studied the free convective heat and mass transfer for

MHD flow over a permeable vertical stretching sheet in the presence of the radiation and buoyancy effects. Bhattacharyya et.al.[7] have investigated the effects of suction/blowing on steady boundary layer stagnation-point flow and heat transfer towards a shrinking sheet with thermal radiation. Many processes in engineering applications occur at high temperatures and the radiate heat transfer becomes very important for the design of the pertinent equipments. However the time-dependent boundary layer flows have been scarcely studied. Rashidi et.al.[42] have presented an analytic approximate solution for unsteady boundary-layer flow and heat transfer due to a stretching sheet by Homotopy analysis method. B.J.Gireesha *et al.* [16,17] numerically investigated the boundary Layer flow of an unsteady dusty fluid and heat transfer over a stretching surface with non-uniform heat source/sink. Mohmmod S. *et al.* [32] discussed the unsteady boundary layer rotating flow due to a stretching surface. Mukhopadhyay [36] examined the effect of thermal radiation on the unsteady mixed convection flow and heat transfer bounded by a porous stretching surface embedded in a porous medium. Sharma et.al. [47] have studied unsteady MHD forced convection flow and mass transfer along a vertical stretching sheet with heat source / sink and variable fluid. There have been many theoretical models developed to describe flow properties and heat transfer towards a stretching sheet, but here it is not possible to present all the literatures. So some of the referred papers cited in the reference section. Due to entrainment of the ambient fluid, this boundary layer flow is quite different from Blasius flow past a flat plate. At low temperature, electrification of solid particles occurs because of impact with the wall. Even a very slight charge on the solid particles will have a pronounced effect on concentration distribution in the flow of a gas-solid system. Although electric charge on the solid particles can be excluded by definition in theoretical analysis or when dealing truly with a boundless system, electrification of the solid particles always occurs when contact and separation are made between the solid particles and a wall of different materials or similar materials but different surface condition . Soo [49] . The electric charges on the solid particles cause deposition of the solid particles on a wall in a more significant manner than the gravity effect and are expected to affect the motion of a metalized propellant and its product of reaction through a rocket nozzle and the jet at the exit of the nozzle. The charged solid particles in the jet of a hot gas also effect radio communications. As a general statement, any volume element of charge species, with charge "e" experiences an instantaneous force given by the Lorentz force law,  $\vec{f} = e\vec{E} + \vec{j} \times \vec{B}$ , where  $\vec{B}$  is the magnetic flux density. The current densities in corona discharge are so low that the magnetic force term  $\vec{j} \times \vec{B}$  can be omitted, as this term is many orders of magnitude smaller than the Coulomb term  $e\vec{E}$ . The ion drift motion arises from the interaction of ions, constantly subject to the Lorentz force with the dense neutral fluid medium. This interaction produces an effective drag force on the ions. The drag force is in equilibrium with the Lorentz force so that the ion velocity in a field  $\vec{E}$  is limited to  $k_m\vec{E}$ , where  $k_m$  is the mobility of the ion species. The drag force on the ions has an equal and opposite reaction force acting on the neutral fluid molecules via this ion-neutral molecules interaction, the force on the ions is transmitted

directly to the fluid medium, so the force on the fluid particles is also given by the above equation. But so far to the author's knowledge, the investigators have not considered electrification of particles in their modeling. Further no attempt has been made in the existing scientific literatures for the consideration of the combined effects of thermal radiation and heat generation/absorption with electrification of particles and viscous dissipation. The present modeling has considered the diffusion of particles through the carrier fluid i.e. the random motion of the particles is taken into account because of the small size of the particles. . Here the terms related to the heat added to the system to slip-energy flux in the energy equation of particle phase, The momentum equation for particulate phase in normal direction, heat due to conduction and viscous dissipation in the energy equation of the particle phase have been considered for better understanding of the boundary layer characteristics. The physical-computational difficulties pertaining to inclusion of radiation and electrification of particles, viscous dissipation and source/sink parameters are addressed with reasonable simplification using similarity transformations. The governing partial differential equations are reduced into system of ordinary differential equations and solved by Shooting Technique using Runge-Kutta Method.

**2. Modeling of the problem:**

Here an unsteady two dimensional laminar boundary layer flow of viscous, incompressible dusty fluid over a vertical stretching sheet has been considered. It is assumed that both the fluid and the dust particle clouds are stationary at the beginning as well as the dust particles are spherical in shape and uniform in size throughout the flow field. The flow is caused by impermeable stretching sheet. The sheet is considered along the x-axis in which y-axis is taken as normal. Two equal and opposite forces are applied along the stretching sheet. Let  $U_w(x)$  be the stretched velocity along the x-axis and origin is fixed in the fluid with the free stream temperature  $T_\infty$ .

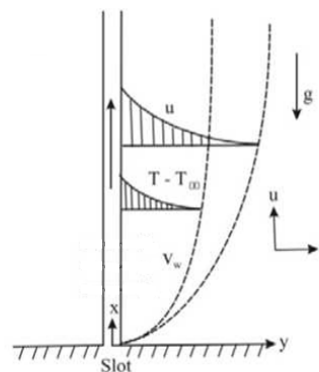


Fig.2.1: Schematic diagram of the flow  
 The governing equations are;

$$\frac{\partial u}{\partial x} + \frac{\partial v}{\partial y} = 0 \tag{2.1}$$

$$\frac{\partial}{\partial t} \rho_p + \frac{\partial}{\partial x} (\rho_p u_p) + \frac{\partial}{\partial y} (\rho_p v_p) = 0 \tag{2.2}$$

$$(1 - \varphi) \rho \left[ \frac{\partial u}{\partial t} + u \frac{\partial u}{\partial x} + v \frac{\partial u}{\partial y} \right] = (1 - \varphi) \mu \frac{\partial^2 u}{\partial y^2} - \frac{1}{\tau_p} \varphi \rho_s (u - u_p) - (1 - \varphi) \rho g \beta^* (T - T_\infty) + \varphi \rho_s \left( \frac{e}{m} \right) E \tag{2.3}$$

$$\varphi \rho_s \left( \frac{\partial u_p}{\partial t} + u_p \frac{\partial u_p}{\partial x} + v_p \frac{\partial u_p}{\partial y} \right) = \frac{\partial}{\partial y} \left( \varphi \mu_s \frac{\partial u_p}{\partial y} \right) + \frac{1}{\tau_p} \varphi \rho_s (u - u_p) + \varphi (\rho_s - \rho) g + \varphi \rho_s \left( \frac{e}{m} \right) E \quad (2.4)$$

$$\varphi \rho_s \left( \frac{\partial v_p}{\partial t} + u_p \frac{\partial v_p}{\partial x} + v_p \frac{\partial v_p}{\partial y} \right) = \frac{\partial}{\partial y} \left( \varphi \mu_s \frac{\partial v_p}{\partial y} \right) + \frac{1}{\tau_p} \varphi \rho_s (v - v_p) \quad (2.5)$$

with boundary conditions

$$u = U_w(x) = \frac{cx}{1-at}, v = 0 \text{ as } y \rightarrow 0$$

$$\rho_p = \omega \rho, u = 0, u_p = 0, v_p \rightarrow v \text{ as } y \rightarrow \infty,$$

where  $\omega$  is the density ratio in the main stream.

### 3. Flow Analysis:

Introducing the following non dimensional variables to solve equations (2.1) to (2.5)

$$u = \frac{cx}{1-at} f'(\eta), v = -\sqrt{\frac{cv}{1-at}} f(\eta), \frac{\varphi \rho_s}{\rho} = \frac{\rho_p}{\rho} = \rho_r =$$

$$H(\eta), u_p = \frac{cx}{1-at} F(\eta), v_p = \sqrt{\frac{cv}{1-at}} G(\eta),$$

$$\eta = \sqrt{\frac{c}{v(1-at)}} y, Pr = \frac{\mu c_p}{k}, \beta = \frac{1-at}{c \tau_p}, \epsilon = \frac{v_s}{v},$$

$$\varphi = \frac{\rho_p}{\rho_s}, A = \frac{a}{c}, E_c = \frac{cv}{c_p T_0}, M = \frac{(1-at)^2}{c^2 x} \left( \frac{e}{m} \right) E,$$

$$Fr = \frac{c^2 x}{g(1-at)^2}, Gr = \frac{g \beta^* (T_w - T_\infty)(1-at)^2}{c^2 x}, \gamma = \frac{\rho_s}{\rho}, \nu = \frac{\mu}{\rho}$$

Obviously the equations (2.1) and (2.5) reduced to following ordinary differential equations

$$H'(\eta) = -(HF + HG') / \left( A \frac{\eta}{2} + G \right) \quad (3.1)$$

$$f''' = -ff'' + (f')^2 + A \left( f' + \frac{\eta}{2} f'' \right)$$

$$-\frac{\beta H}{(1-\varphi)} (F - f') - \frac{HM}{(1-\varphi)} - Gr \theta(\eta) \quad (3.2)$$

$$F'' = \left[ \begin{array}{c} A \left\{ \frac{\eta}{2} F' + F \right\} + (F')^2 + GF' + \beta (F - f') \\ - \left( 1 - \frac{1}{\gamma} \right) \frac{1}{Fr} - M \end{array} \right] / \epsilon \quad (3.3)$$

$$G'' = \left[ \frac{A}{2} (\eta G' + G) + GG' + \beta (f + G) \right] / \epsilon \quad (3.4)$$

With boundary conditions

$$G' = 0, f = 0, f' = 1, F' = 0 \text{ as } \eta \rightarrow 0$$

$$f' = 0, F = 0, G = -f, H = \omega \text{ as } \eta \rightarrow \infty$$

### 4. Heat transfer analysis:

The governing temperature equations are;

$$(1 - \varphi) \rho c_p \left[ \frac{\partial T}{\partial t} + u \frac{\partial T}{\partial x} + v \frac{\partial T}{\partial y} \right]$$

$$= (1 - \varphi) k \frac{\partial^2 T}{\partial y^2} + \frac{1}{\tau_r} \varphi \rho_s c_s (T_p - T)$$

$$+ \frac{1}{\tau_p} \varphi \rho_s (u - u_p)^2 + (1 - \varphi) \mu \left( \frac{\partial u}{\partial y} \right)^2$$

$$+ \varphi \rho_s \left( \frac{e}{m} \right) E u_p - (1 - \varphi) \frac{\partial q_r}{\partial y} + (1 - \varphi) q''' \quad (4.1)$$

$$\varphi \rho_s c_s \left[ \frac{\partial T_p}{\partial t} + u_p \frac{\partial T_p}{\partial x} + v_p \frac{\partial T_p}{\partial y} \right]$$

$$= \frac{\partial}{\partial y} \left( \varphi k_s \frac{\partial T_p}{\partial y} \right) - \frac{1}{\tau_p} \varphi \rho_s c_s (T_p - T)$$

$$- \frac{1}{\tau_p} \varphi \rho_s (u - u_p)^2 + \varphi \mu_s \left[ u_p \frac{\partial^2 u_p}{\partial y^2} + \left( \frac{\partial u_p}{\partial y} \right)^2 \right] +$$

$$\varphi \rho_s \left( \frac{e}{m} \right) E u_p - \varphi \frac{\partial q_{rp}}{\partial y} + \varphi q_p''' \quad (4.2)$$

In order to solve the temperature equations (4.1) and (4.2), we consider the non-dimensional temperature boundary conditions as follows;

$$T = T_w = T_\infty + T_0 \frac{cx^2}{v(1-at)^2} \text{ at } y = 0$$

$$\text{and } T \rightarrow T_\infty, T_p \rightarrow T_\infty \text{ as } y \rightarrow \infty$$

$$\text{For most of the gases } \tau_p \approx \tau_T, k_s = k \frac{c_s \mu_s}{c_p \mu} \text{ if } \frac{c_s}{c_p} = \frac{2}{3Pr}$$

Rosseland approximation is assumed to account for radiate heat flux in presence of electrification of particles in the flow with internal heat generation/absorption. Using Rosseland approximation, the radiate e heat flux  $q_r$  is modeled as:

$$q_r = -\frac{4\sigma^* \partial T^4}{3k^* \partial y}, \text{ where } \sigma^* \text{ is the Stefan-Boltzman constant and } k^* \text{ is the mean absorption coefficient.}$$

Assuming that the differences in the temperature within the flow to be sufficiently small so that  $T^4$  can be expressed as linear function of the temperature, one can expand  $T^4$  in a Taylor's series about  $T_\infty$  as follows

$$T^4 = T_\infty^4 + 4T_\infty^3(T - T_\infty) + 6T_\infty^2(T - T_\infty)^2 + \dots$$

By neglecting higher order terms beyond the first degree in  $(T - T_\infty)$  we get:

$$T^4 = -3T_\infty^4 + 4T_\infty^3 T$$

Substituting this value in  $q_r$ , we get

$$\frac{\partial q_r}{\partial y} = -\frac{16T_\infty^3 \sigma^* \partial^2 T}{3k^* \partial y^2}$$

Similarly for particle phase, we can write

$$\frac{\partial q_{rp}}{\partial y} = -\frac{16T_\infty^3 \sigma^* \partial^2 T_p}{3k^* \partial y^2}$$

Introducing the following non dimensional variables in equation (4.1) to (4.2)

$$q''' = \left( \frac{kU_w(x)}{xv} \right) [A^*(T_w - T_\infty) f'(\eta) + B^*(T - T_\infty)]$$

$$q_p''' = \left( \frac{kU_w(x)}{xv} \right) [A^*(T_w - T_\infty) F(\eta) + B^*(T_p - T_\infty)],$$

$$\theta(\eta) = \frac{T - T_\infty}{T_w - T_\infty}, \theta_p(\eta) = \frac{T_p - T_\infty}{T_w - T_\infty}, Ra = \frac{16T_\infty^3 \sigma^*}{3kk^*}$$

$$\text{Where } T - T_\infty = T_0 \frac{cx^2}{v} \frac{1}{(1-at)^2} \theta,$$

$$T_p - T_\infty = T_0 \frac{cx^2}{v} \frac{1}{(1-at)^2} \theta_p.$$

The temperature equations are reduced into the following forms:

$$\theta'' = \frac{\left[ Pr(2f'\theta - f\theta') - \frac{2}{3} \frac{\beta H}{1-\varphi} (\theta_p - \theta) - \frac{Pr E_c \beta H}{1-\varphi} (F - f')^2 - Pr E_c (f'')^2 \right] + \frac{A}{2} Pr (\eta \theta'(\eta) + 4\theta(\eta)) - \frac{Pr E_c H M F(\eta)}{(1-\varphi)} - (A^* f'(\eta) + B^* \theta(\eta))}{(1 + Ra)} \quad (4.3)$$

$$\theta_p'' = \frac{\left[ \frac{A}{2} (\eta \theta_p' + 4\theta_p) + 2F\theta_p + G\theta_p' + \beta(\theta_p - \theta) + \frac{3}{2} E_c Pr \beta (f' - F)^2 \right] - \frac{3}{2} \epsilon E_c Pr (FF' + (F')^2) - \frac{3}{2} E_c Pr M F - \frac{3}{2} \frac{1}{\gamma} (A_p^* F(\eta) + B_p^* \theta_p(\eta))}{\left( \frac{\epsilon}{Pr} + \frac{3}{2} Ra \right)} \quad (4.4)$$

With boundary condition

$$\theta = 1, \theta_p' = 0 \text{ as } \eta \rightarrow 0$$

$$\theta \rightarrow 0, \theta_p \rightarrow 0 \text{ as } \eta \rightarrow \infty$$

### 5. Calculation of skin friction coefficient and local Nusselt number:

The physical quantities of interest are the skin friction coefficient  $C_f$  and the local Nusselt number  $Nu_x$  which are defined as  $C_f = \frac{\tau_w}{\rho U_w^2}, Nu_x = \frac{xq_w}{k(T_w - T_\infty)}$ , where the surface shear stress  $\tau_w$  and surface heat flux  $q_w$  are given by  $\tau_w = \mu \left( \frac{\partial u}{\partial y} \right)_{y=0}, q_w = -k \left( \frac{\partial T}{\partial y} \right)_{y=0}$

### 6. Solution Method:

The set of non-linear differential Equations (3.1) to (3.4), (4.3) and (4.4) subject to the boundary conditions were solved numerically using Runge-Kutta method with shooting technique. The advantage of shooting technique is to solve a boundary value problem by converting it into initial value problem. Here in this problem the values of  $f''(0), F(0), G(0), H(0), \theta'(0)$  and  $\theta_p(0)$  are not known but  $f'(\infty) = 0, F(\infty) = 0, G(\infty) = -f(\infty), H(\infty) = \omega, \theta(\infty) = 0, \theta_p(\infty) = 0$  are given. We use Shooting method to determine the values of  $f''(0), F(0), G(0), H(0), \theta'(0), \theta_p(0)$ . In this problem the missing values of  $f''(0), \theta'(0), F(0), G(0), H(0)$  and  $\theta_p(0)$  for different set of values of parameter are chosen on hit and trial basis such that the boundary condition at other end i.e. the boundary condition at infinity ( $\eta_\infty$ ) are satisfied. The most important step in this method is to choose an appropriate finite value of  $\eta \rightarrow \infty$ . In order to determine  $\eta \rightarrow \infty$  for the boundary value problem described by Equations (3.1) to (3.4), (4.3) and (4.4), we start with initial guess values for a particular set of physical parameters to obtain  $F(0), G(0), H(0), \theta_p(0), \theta'(0)$  and  $f''(0)$ . The solution procedure is repeated with another large value of  $\eta \rightarrow \infty$  until two successive values of  $F(0), G(0), H(0), \theta_p(0), \theta'(0)$  and  $f''(0)$  differ only by a specified significant digit. We have supplied  $f''(0) = \alpha_0$  and  $f''(0) = \alpha_1$ . The improved value of  $f''(0) = \alpha_2$  is determined by utilizing linear interpolation formula. Then the value of  $f'(\alpha_2, \infty)$  is determined by using Runge-Kutta method. If  $f'(\alpha_2, \infty)$  is equal to  $f'(\infty)$  up to a certain decimal accuracy, then  $\alpha_2$  i.e.  $f''(0)$  is determined, otherwise the above procedure is continued with  $\alpha_0 = \alpha_1$  and  $\alpha_1 = \alpha_2$  until a correct  $\alpha_2$  is obtained. The same procedure described above is adopted to determine the correct values of  $F(0), G(0), H(0), \theta'(0), \theta_p(0)$ . If they agreed to about six significant digits, the last value of  $\eta_\infty$  is used; otherwise the procedure is repeated until further change in  $\eta_\infty$  did not lead to any more change in the value of  $F(0), G(0), H(0), \theta_p(0), \theta'(0)$  and  $f''(0)$ . Depending upon the initial guess and number of steps  $N=81.0$ , the solution of the present problem is obtained by numerical computation after finding the infinite value for  $\eta$ . So we ran our bulk of computations for  $\eta_\infty = 5.0$  with step size  $\Delta\eta = 0.125$ . The value of  $\eta$  may change for a different set of physical parameters. It has been observed from the numerical result that the approximation to  $F(0), G(0), H(0), \theta_p(0), \theta'(0)$  and  $f''(0)$  are improved by increasing the infinite value of  $\eta$  which is finally determined as  $\eta = 5.0$  with a step length of  $\Delta\eta = 0.125$  beginning from  $\eta = 0$  to ensure to be the satisfactory convergence criterion of  $1 \times 10^{-6}$  to achieve the far field boundary conditions asymptotically for all values of the parameters considered. For the sake of brevity further details on the solution process are not presented here. It is also important to note that the computational time for each set of input parameter values should be short. Because physical domain in this problem is unbounded, whereas the computational domain has to be finite, we apply the far field boundary conditions for the similarity variable  $\eta$  at finite value denoted by  $\eta_\infty$  and the solutions are obtained with an error tolerance of  $10^{-6}$  in all the cases. The accuracy of the numerical scheme has been validated by comparing the skin friction and the wall temperature gradient results to those reported in the

previous studies. The following table shows an excellent agreement between our numerical results and the previously reported results. The accuracy of results obtained by our investigation is compared with the results obtained by Chen C.H [8], Grubka et.al.[19], Subhas et.al.[50], Mukhopadhaya et.al.[36], Ishak et.al.[21] and Gireesha et.al.[16,17] for the local nusselt number in the limiting condition  $\beta, A^*, B^*, A_p^*, B_p^*, R_a, G_r, E_c, A, M, \phi = 0.0$  which is shown in "Table-1". It is observed from the table that our result is good agreement with their results.

**7. Discussion of Result:**

The computations were done by the computer language FORTRAN-77. The shear stress (Skin friction coefficient) which is proportional to  $f''(0)$  and rate of heat transfer (Nusselt number) which is proportional to  $\theta'(0)$  are tabulated in "Table-2" for different values of parameters used. It is observed from the table that shear stress and rate of heat transfer decrease on the increase of 'Ec'. The shear stress and rate of heat transfer increase for increasing values of Pr. The Nusselt number increases on the increasing values of unsteady parameter 'A' and electrification parameter 'M', but Nusselt number decreases when the radiation parameter 'Ra' increases. The skin friction coefficient decreases for increasing value of 'M'. It is also observed from the table that the increasing value of diffusion parameter  $\epsilon$  decrease both the skin friction and Nusselt number.

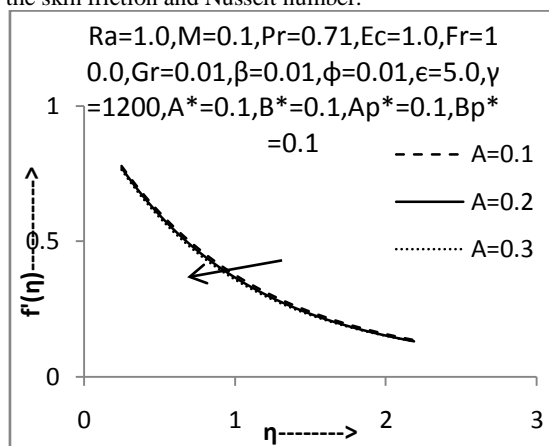


Fig.1: Non-dimensional velocity profile of fluid phase w.r.t. 'A'

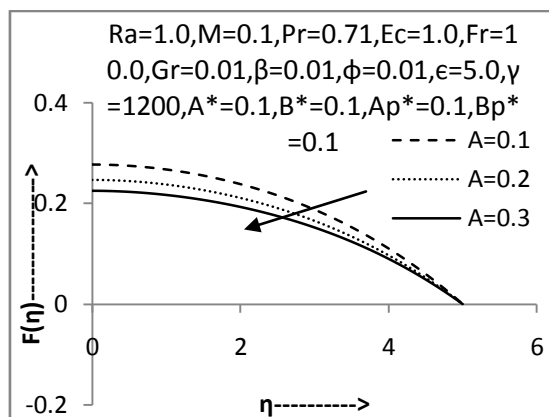


Fig.2: Non-dimensional velocity profile of particle phase w.r.t. 'A'

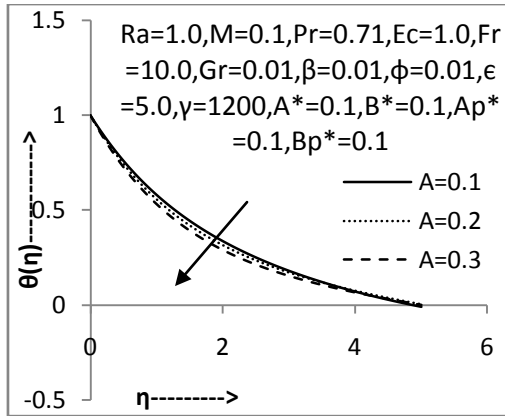


Fig.3: Non-dimensional temperature profile of fluid phase w.r.t. 'A'

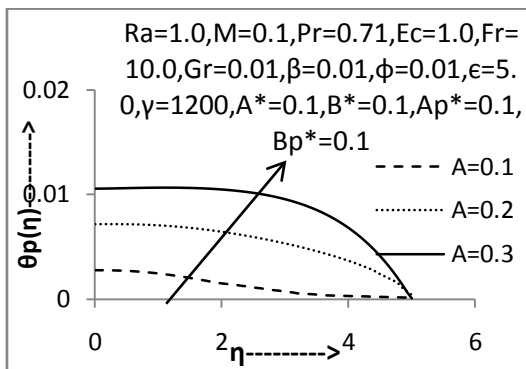


Fig.4: Non-dimensional temperature profile of particle phase w.r.t. 'A'

“Fig-1” and “Fig-2” demonstrate the velocity profile of fluid phase and particle phase respectively. It is observed that the velocity of both phases decrease on the increase of unsteady parameter ‘A’. This is because of fluid flow caused by stretching sheet. “Fig-3” explains that the temperature of fluid phase decreases with increasing of unsteady parameter ‘A’. Physically, when the unsteadiness increases the sheet loses more heat which causes decrease in temperature. We also observe that as the distance from the stretching sheet within dynamic region increases, temperature field decreases as unsteadiness increases. But “Fig -4” describes that the temperature profile of particle phase increases on the increase of unsteady parameter because getting more time of collision of particles produce more frictional heating.

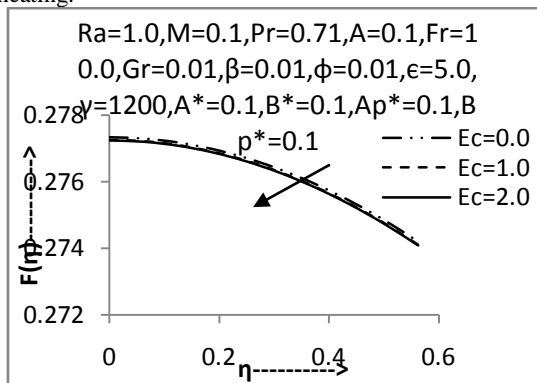


Fig.5: Non-dimensional velocity profile of particle phase w.r.t. 'Ec'

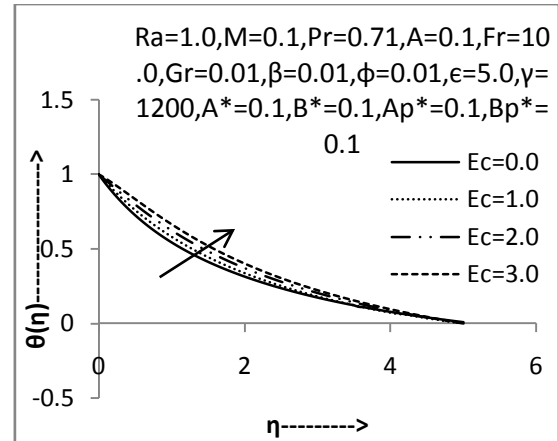


Fig.6: Non-dimensional temperature profile of fluid phase w.r.t. 'Ec'

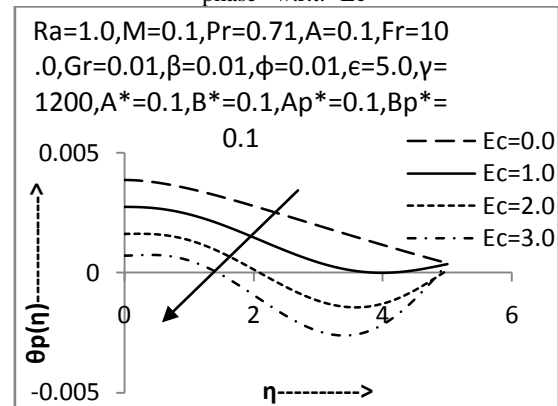


Fig.7: Non-dimensional temperature profile of particle phase w.r.t. 'Ec'

“Fig-5” depicts the velocity profile of particle phase which shows that the increasing value of Ec decreases the velocity profile of particle phase. “Fig-6” explain that the increasing values of Ec, increases the temperature of fluid phase because the large values of Ec give rise to a strong viscous dissipation effect as a result the heat energy is stored in the fluid which enhances the temperature and thermal boundary layer thickness, but the “Fig-7” shows that increasing values of Ec, decrease the temperature of particle phase.

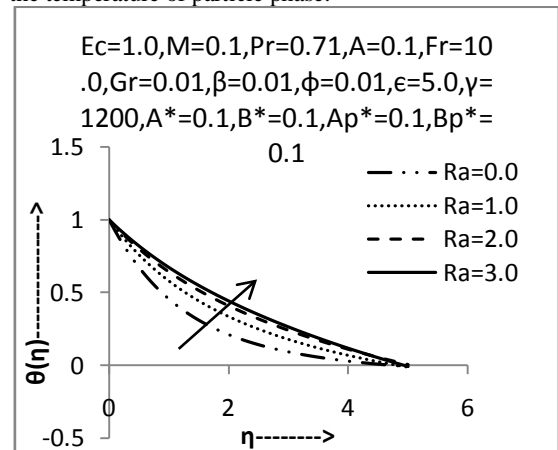


Fig.8: Non-dimensional temperature profile of fluid phase w.r.t. 'Ra'

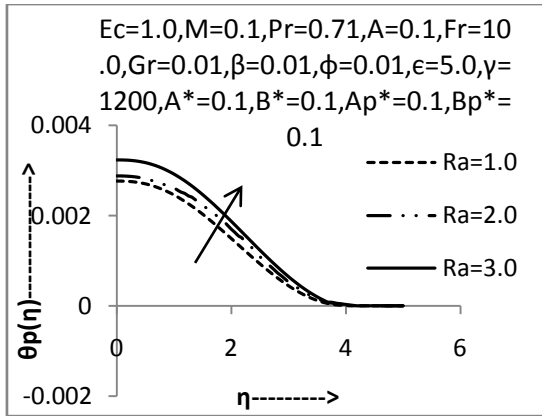


Fig.9: Non-dimensional temperature profile of particle phase w.r.t. 'Ra'

“Fig-8” and “Fig-9” depict the variation of temperature of fluid phase and particle phase respectively. It is observed that the enhancing value of Radiation parameter ‘Ra’ enhances significantly the temperature of both fluid phase and particle phase. This is due to the fact that the divergences of the radiate heat flux increases as the Rosseland radiate absorption  $k^*$  diminishes which in turn increases the rate of radiate heat transfer to the fluid. Thus the presence of thermal radiation enhances thermal state of the fluid causing its temperature to increase. It means the thermal boundary layer thickness is increasing on the increase of radiation parameter.

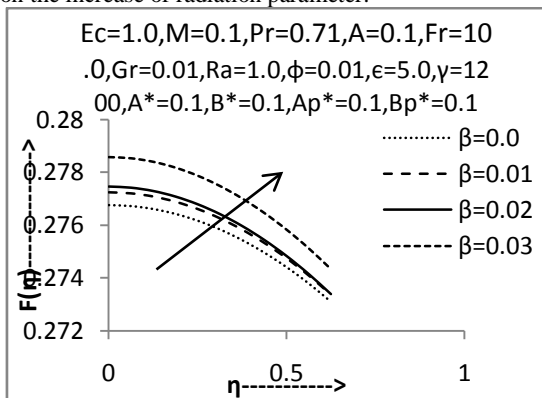


Fig.10: Non-dimensional velocity profile of particle phase w.r.t. ‘β’

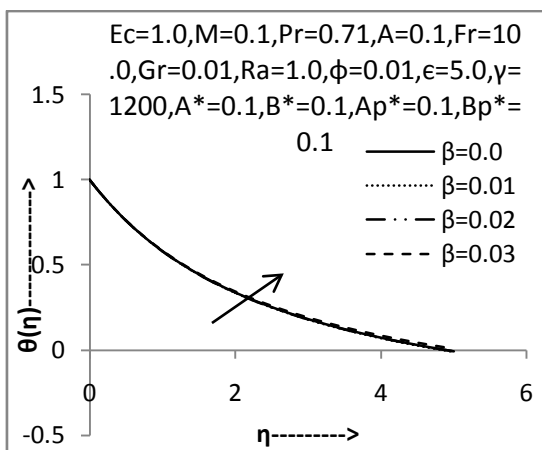


Fig.11: Non-dimensional temperature profile of fluid phase w.r.t. ‘β’

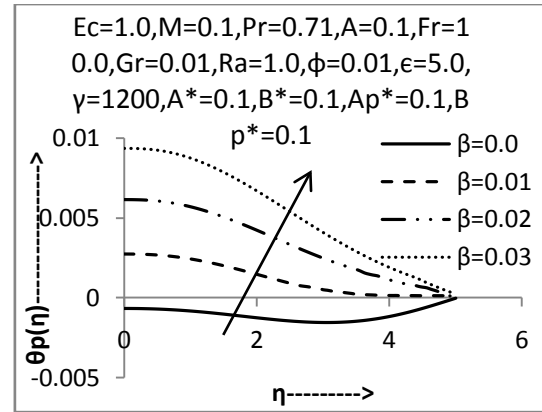


Fig.12: Non-dimensional temperature profile of particle phase w.r.t. ‘β’

“Fig-10” demonstrates the effect of  $\beta$  which infers that increasing of  $\beta$  increases the particle phase velocity. “Fig-11” and “Fig-12” illustrate that the increasing of  $\beta$  increases the temperature of both fluid as well as particle phase because delaying the accumulation of high volume fractions of particles allows greater access of the fluid to the particles increase the convective heat and mass transfer.

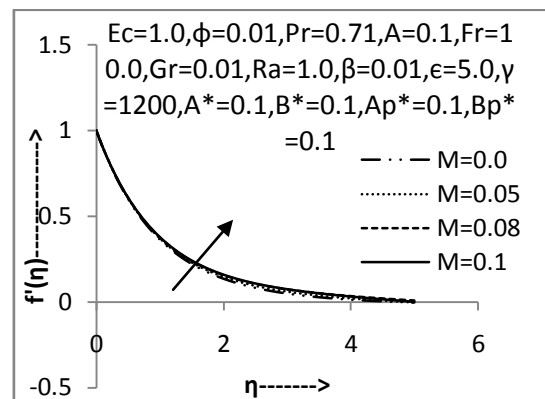


Fig.13: Non-dimensional velocity profile of fluid phase w.r.t. ‘M’

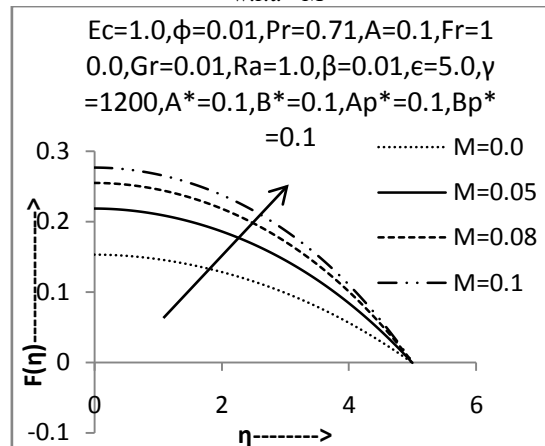


Fig.14: Non-dimensional velocity profile of particle phase w.r.t. ‘M’

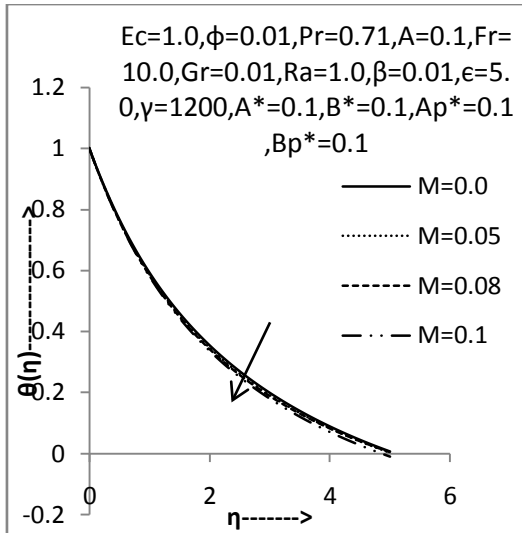


Fig.15: Non-dimensional temperature profile of fluid phase w.r.t. 'M'

"Fig-13" and "Fig-14" represent the increase of Electrification parameter 'M' increase the velocity of both fluid phase and particle phase respectively. "Fig-15" demonstrates the temperature of fluid phase. It is noticed that the temperature of fluid phase decrease with increase of Electrification parameter 'M' due to the applied transverse electric field opposing the motion.

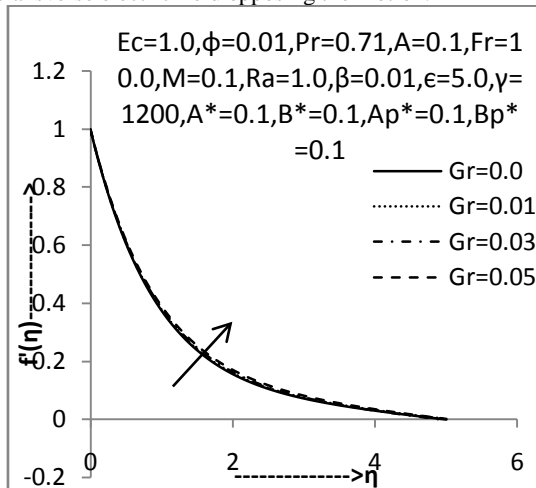


Fig.16: Non-dimensional velocity profile of fluid phase w.r.t. 'Gr'

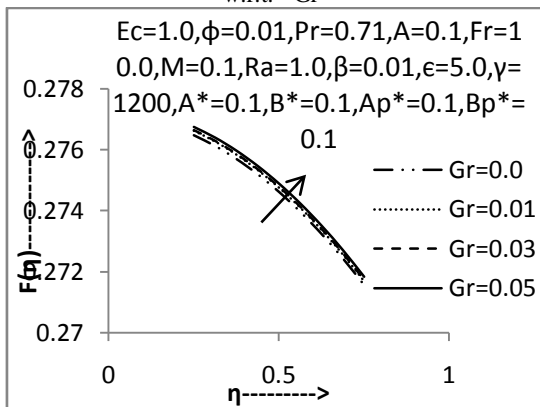


Fig.17: Non-dimensional velocity profile of fluid phase w.r.t. 'Gr'

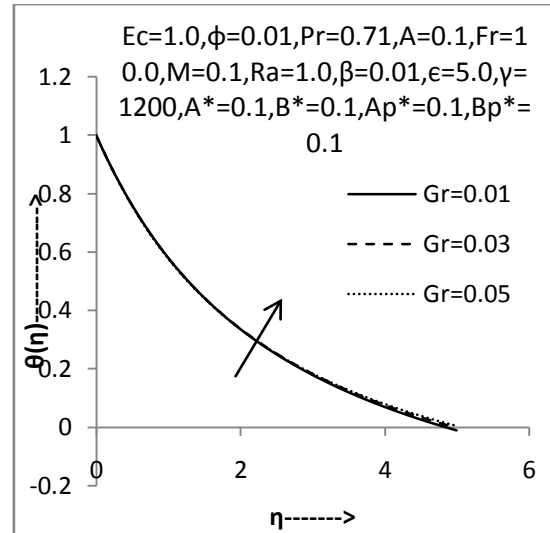


Fig.18: Non-dimensional temperature profile of fluid phase w.r.t. 'Gr'

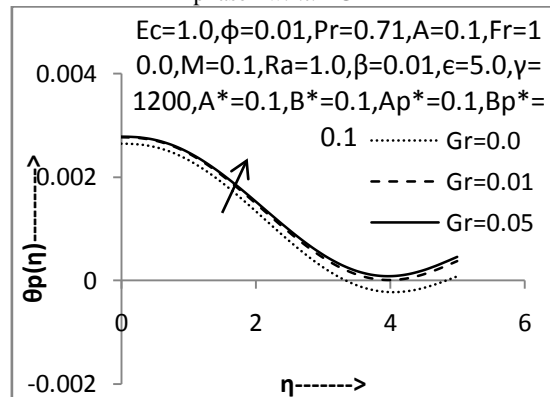


Fig.19: Non-dimensional temperature profile of particle phase w.r.t. 'Gr'

Effects of Grashof number Gr exhibit the velocity profile of both fluid and particle phase in "Fig-16" and "Fig-17" respectively. Since the flow is accelerated due to the enhancement in buoyancy force corresponding to an increasing in the Gr, as a result the thermal influences the velocity within the boundary layer, so velocity increases. "Fig-18" and "Fig-19" are obtained for temperature profiles of both phases by the numerical simulation of various values of Gr. Temperature profiles illustrate that the temperature are increased due to increase of Gr.

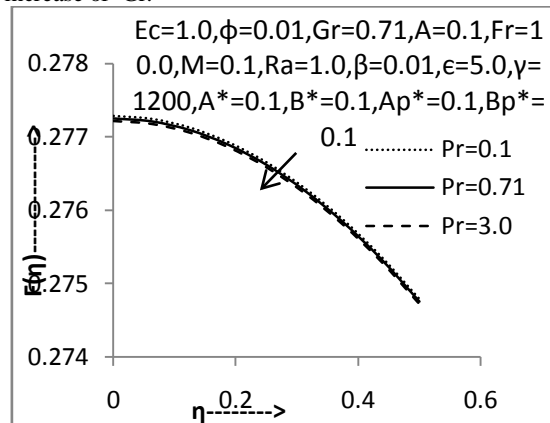


Fig.20: Non-dimensional velocity profile of particle phase w.r.t. 'Pr'

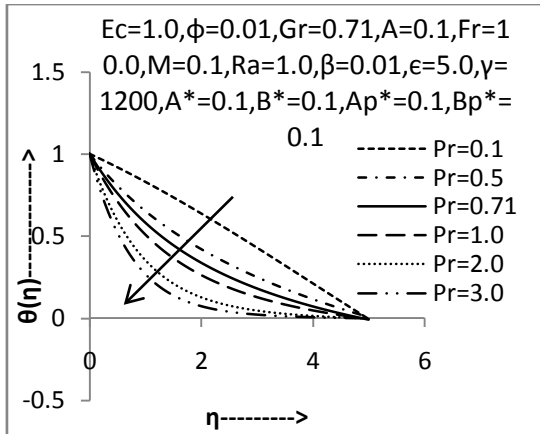


Fig.21: Non-dimensional temperature profile of fluid phase w.r.t. 'Pr'

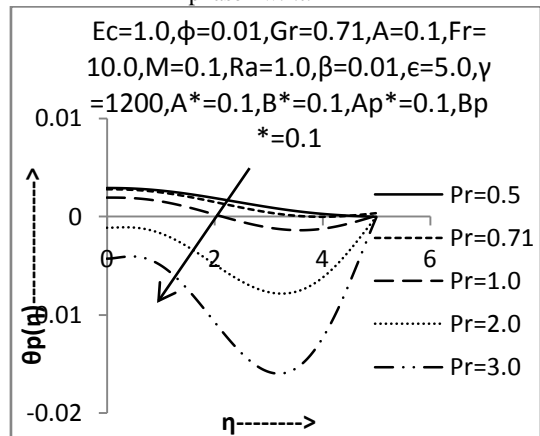


Fig.22: Non-dimensional temperature profile of particle phase w.r.t. 'Pr'

"Fig-20" indicates the increase of velocity profile particle phase with increase of Pr. "Fig-21" and "Fig-22" depicts the effect of Pr on temperature profile of fluid phase and particle phase. From the figure we observe that, when Pr increases the temperature of both phases decreases. This is due to the fact that for smaller values of Pr are equivalent to larger values of thermal conductivities, this phenomenon leads to the decreasing of energy ability that reduces the thermal boundary layer and therefore heat is able to diffuse away from the stretching sheet.

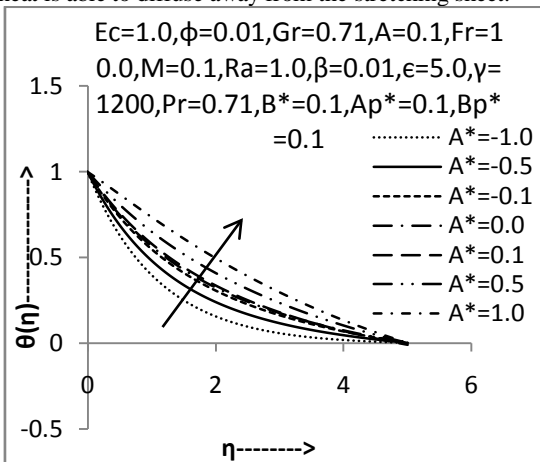


Fig.23: Non-dimensional temperature profile of fluid phase w.r.t. 'A\*'

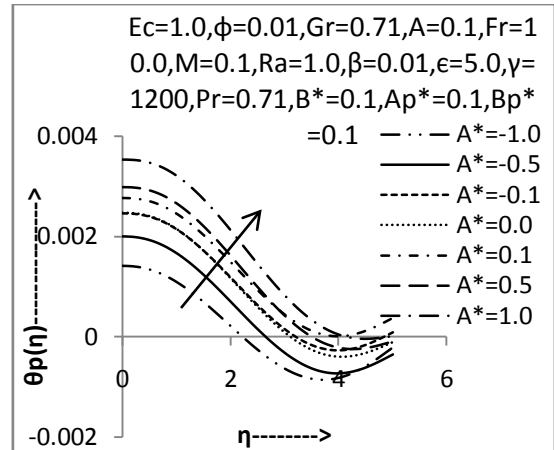


Fig.24: Non-dimensional temperature profile of particle phase w.r.t. 'A\*'

"Fig-23" and "Fig-24" demonstrates that the temperature of both phases increase with increasing value of A\*. Because the presence of the heat source generates energy in the thermal boundary layer and as a consequence the temperature rises. In the case of heat absorption A\* < 0 the temperature falls with decreasing values of A\* < 0 owing to the absorption of energy in the boundary layer.

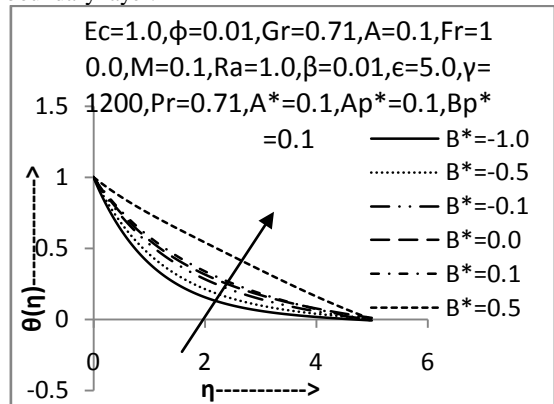


Fig.25: Non-dimensional temperature profile of fluid phase w.r.t. 'B\*'

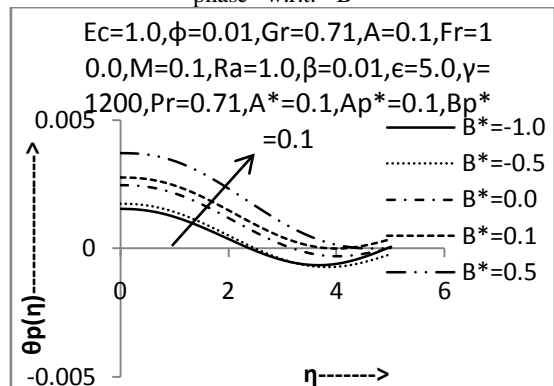


Fig.26: Non-dimensional temperature profile of particle phase w.r.t. 'B\*'

"Fig-25" and "Fig-26" explains the behavior of temperature of both phases w.r.t. B\* which indicates that the increase value of B\* increase the temperature of both phases. As in the case of space dependent heat source the temperature increases due to the release of thermal energy for B\* > 0 while the temperature drops for B\* < 0



decreasing values of  $B^* < 0$  owing to the absorption of energy.

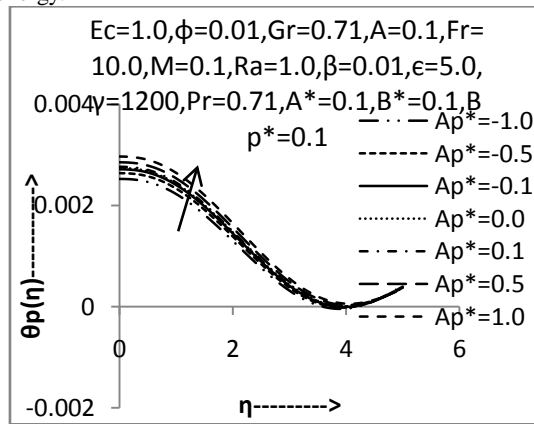


Fig.27: Non-dimensional temperature profile of particle phase w.r.t. 'Ap\*'.

“Fig-27” demonstrates that the temperature of fluid phases increase with increasing value of  $Ap^*$ . Because the presence of the heat source generates energy in the thermal boundary layer and as a consequence the temperature rises. In the case of heat absorption  $Ap^* < 0$  the temperature falls with decreasing values of  $Ap^* < 0$  owing to the absorption of energy in the boundary layer.

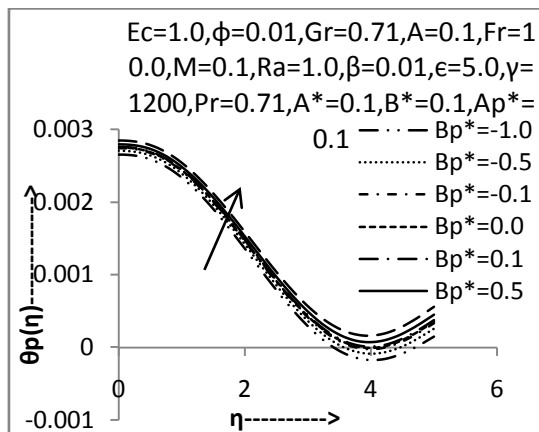


Fig.28: Non-dimensional temperature profile of particle phase w.r.t. 'Bp\*'.

“Fig-28” demonstrates that the temperature of particle phases increase with increasing value of  $Bp^*$ . As in the case of space dependent heat source the temperature increases due to the release of thermal energy for  $Bp^* > 0$  while the temperature drops for decreasing values of  $Bp^* < 0$  owing to the absorption of energy.

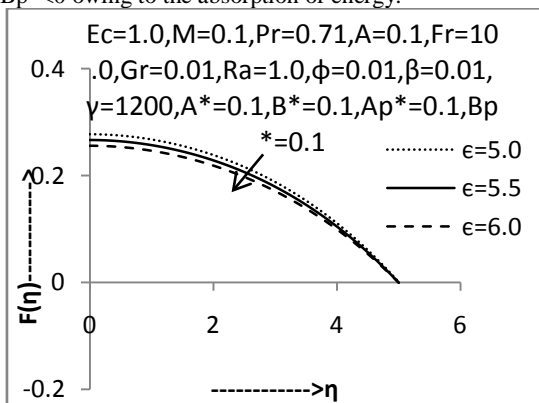


Fig.29: Non-dimensional velocity profile of particle phase w.r.t.  $\epsilon$ .

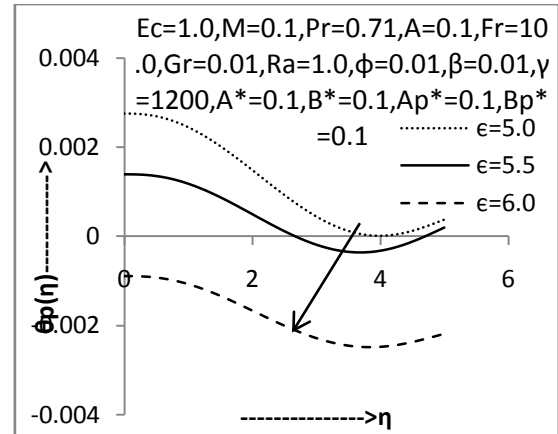


Fig.30: Non dimensional temperature profile of particle phase w.r.t 'epsilon'.

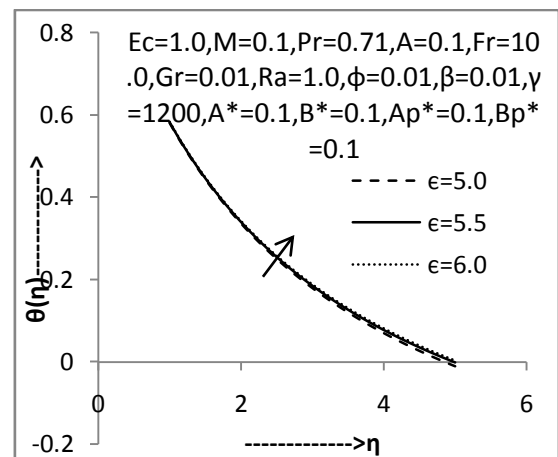


Fig.31: Non dimensional temperature profile of fluid phase w.r.t 'epsilon'.

“Fig-29” shows the effect of  $\epsilon$  on velocity of particle phase. It is evident from figure that the increasing values of  $\epsilon$  decreases the velocity of particle phase. When the length increases the driving force decreases as we approach equilibrium and this lowers the mass transfer coefficient. “Fig-30” shows the temperature of particle phase decrease with the increase value of  $\epsilon$  due to heat transfer from particle phase to fluid phase. “Fig-31” witnesses the increase of temperature of fluid phase with the increasing value of  $\epsilon$ . Because, when the particles diffuse through the fluid, the particle-particle interaction produces more frictional heating.

### 5. Conclusions:

We concluded by noting that the boundary layer flow and heat transfer characteristics have been discussed extensively by considering various physical parameters like unsteady parameter 'A', Prandtl number 'Pr', Eckert number 'Ec', Electrification parameter 'M', Radiation parameter 'Ra', Grashof Number 'Gr', heat source/sink parameters  $A^*$  and  $B^*$ , volume fraction ' $\phi$ ' and particle interaction parameter ' $\beta$ ', ratio of specific heat  $\gamma$ , diffusion parameter ' $\epsilon$ ', Froude number 'Fr'. The novelty of the study is the consideration of electrification of particles and diffusion parameter that are scarcely investigated by other researchers. Our model based on the motion and collisions of particles, as well as the charge transfer during these collisions. Here the focus is made on the role of the inter particle electrostatic forces which has given less attention by other investigators. In

our study the claim is that the velocity profile increases on the increase of electrification parameter which arises due to electrification of particles, whereas, the analysis made by other investigators taking electrically conducting fluid in presence of external magnetic field shows a decrease in fluid velocity due to presence of opposing Lorentz force. It is observed that the increasing values of  $\epsilon$  decreases the velocity of particle phase. As the length increases the driving force decreases as we approach equilibrium and this lowers the mass transfer coefficient. But the temperature of fluid phase increase with the increasing value of  $\epsilon$ , because the diffusion of particles through the fluid produce the frictional heating due to collision of particles. Also the temperature of particle phase decrease with the increase value of  $\epsilon$  due to heat transfer from particle phase to fluid phase. Another important investigation of the present study is the inclusion of radiation term and heat source/sink term in particle phase. The influence of these terms are same as that of fluid phase which has interpreted in detail. The increasing value of unsteady parameter  $A$  decreases the temperature profiles of fluid phase and increase the temperature of dust phase. Also increase value of  $A$  decreases velocity of both phases. The rate of cooling is much faster for higher values of unsteady parameter but it takes long times for cooling during the steady flow. Though the computations are cumbersome due to the consideration of many parameters, but consideration of all these parameters may give a new dimension to the study of stretching sheet problems.

Finally, we observed the following results:

- i. The increasing value of unsteady parameter  $A$  decreases the temperature profiles of fluid phase and increase the temperature of dust phase. Also increase value of  $A$  decreases velocity of both phases.
- ii. The temperature profile of both phases increase with the increase of radiation parameter  $R_a$ . Thus the radiation should be at minimum in order to facilitate the cooling process.
- iii. Increasing value of  $Ec$  is enhancing the temperature of both fluid phase but decrease the temperature of particle phase which indicates that the heat energy is generated in fluid due to frictional heating.
- iv. The thermal boundary layer thickness decreases on the effect of  $Pr$ . The temperature decreases at a faster rate for higher values of  $Pr$  which implies the rate of cooling is faster in case of higher prandtl number.
- v. The thermal boundary layer thickness for fluid phase and momentum boundary layer thickness for both phases are increasing for increased values of electrification parameter  $M$ .
- vi. Increasing  $\beta$  increase the velocity and temperature of the particle phase.
- vii. The momentum boundary layer thickness of both phases increase for the increasing values of  $Gr$  but the thermal boundary layer thickness of fluid phase increases but thermal boundary layer thickness of dust phase decreases for the enhanced value of  $Gr$ .
- viii. Thermal boundary layer thickness of fluid phase increases but thermal boundary layer thickness of dust phase decreases for the enhanced value of  $\epsilon$ .
- ix. We have investigated the problem assuming the values  $\gamma=1200.0, Fr_r = 10.0$

#### References:

- [1]. Adhikari A. and Sanyal D.C. (2013), "Heat transfer on MHD viscous flow over a stretching sheet with prescribed heat flux", Bulletin of International Mathematical Virtual Institute, ISSN 1840-4367, Vol.3, 35-47.
- [2]. Ahmed S., Chamkha A. J. (2010), "Effects of chemical reaction, heat and mass transfer and radiation on mhd flow along a vertical porous wall in the present of induced magnetic field", Int. J. Industrial Mathematics 2, 245-261.
- [3]. Akyildiz T., Siginer D.A., Vajravelu K., Cannon J.R. and Van Gorder R.A. (2010), Similarity solutions of the boundary layer equations for a nonlinearly stretching sheet, Math. Methods Appl Sci. Vol. 33, 601-606.
- [4]. Ali Mohammad, Abdul Alim Md., and Alam Mohammad Shah (2014), "Heat transfer boundary layer flow past an inclined stretching sheet in presence of magnetic field", international Journal of Advancements in Research & Technology, Volume 3, Issue 5, 34, ISSN 2278-7763.
- [5]. Aziz M., Ahmed W., Abbasi M., and Taj, M. (2014), "MHD flow of a viscous fluid over an exponentially stretching sheet in a porous medium," J. Appl. Math., Article ID 256761, 8 pages.
- [6]. Barik R.N., Dash G.C. and Rath P.K. (2012), "Heat and mass transfer on MHD flow through a porous medium over a stretching surface with heat source", Mathematical Theory and Modeling, ISSN 2224-5804, Vol.2, No.7.
- [7]. Bhattacharyya K., Layek G.C. (2011), "Effects of suction/blowing on steady boundary layer stagnation-point flow and heat transfer towards a shrinking sheet with thermal radiation". Int. J. Heat Mass Transf. 54, 302-307
- [8]. Chen C.H. (1998), "Laminar Mixed convection Adjacent to vertical continuity stretching sheet". Heat and Mass Transfer, vol.33, No.5-6, 471-476.
- [9]. Cortell R. (2005), "A note on MHD flow of a power law fluid over a stretching sheet", Appl. Math. Comput. 168, 557-566.
- [10]. Crane L.J. (1970), "Flow past a stretching plate", Zeitschrift fur Angewandte Mathematik und physic ZAMP, VOL.2, NO.4, 645-647.
- [11]. Das M., Mahathal B. K., Nandkeolyar R., Mandal B. K. and Saurabh K. (2014) "Unsteady Hydromagnetic Flow of a Heat Absorbing Dusty Fluid Past a Permeable Vertical Plate with Ramped Temperature" Journal of Applied Fluid Mechanics, Vol. 7, No. 3, pp. 485-492.
- [12]. Datta N. and Mishra S.K. (1982), "Boundary layer flow of a dusty fluid over a semi-infinite flat plate", Acta Mechanica, vol.42, no1-2, 71-83. doi:10.1007/BF01176514
- [13]. Dessie Hunegnaw and Kishan Naikoti (2014), Scaling group analysis on MHD Free convective heat and mass transfer over a stretching surface with suction/injection, heat

- source /sink considering viscous dissipation and chemical reaction effects, *Application and Applied mathematics*, Vol:9, Issue, pp: 553-572, Hunegnawd@yahoo.com, kishan\_n@rediffmail.com
- [14]. Dimian, M.F. and Megahed (2013), A. M., "Effects of variable fluid properties on unsteady heat transfer over a stretching surface in the presence of thermal radiation," *Ukr. J. Phys.* 58, pp. 345.
- [15]. Fang T., Zhang J. and Zhong Y. (2012), "Boundary layer flow over a stretching sheet with variable thickness". *Applied Mathematics and Computation* 218, 7241-7252.
- [16]. Gireesha B.J., Chamakha A.J., Manjunatha S and Bagewadi C.S. (2013), "Mixed convective flow of a dusty fluid over a vertical stretching sheet with non-uniform heat source/sink and radiation"; *International Journal of Numerical Methods for Heat and Fluid flow*, vol.23.No.4,598-612.
- [17]. Gireesha B.J., Roopa G.S. and Bagewadi C.S. (2011), "Boundary Layer flow of an unsteady Dusty fluid and Heat Transfer over a stretching surface with non-uniform heat source/sink", *Engineering*, 3, 726-735, <http://www.SciRP.org/Journal/am>, Scientific Research.
- [18]. Gireesha, B.J. Manjunatha S. and Bagewadi C.S. (2014), "Effect of radiation on boundary layer flow and heat transfer over a stretching sheet in the presence of a free stream velocity", *Journal of Applied fluid Mechanics*, Vol.7, No.1, 15-24.
- [19]. Grubka L.J. and Bobba K.M. (1985), "Heat Transfer characteristics of a continuous stretching surface with variable temperature", *Int.J.Heat and Mass Transfer*, vol.107, 248-250.
- [20]. Hayat T., Farooq M., Alsaedi A., and Falleh Al-Solamy (2016), Impact of Cattaneo-Christov heat flux in the flow over a stretching sheet with variable thickness, <http://dx.doi.org/10.1063/1.4929523>, AIP publishing.
- [21]. Ishak A., Nazar R. and Pop I. (2008), "Hydromagnetic flow and heat transfer adjacent to a stretching vertical sheet", *Heat and Mass Transfer*, Vol. 44, 921-927.
- [22]. Jadav Konch and Hazarika (2016), Effects of Variable Viscosity and Thermal Conductivity on MHD Free Convection Flow of Dusty Fluid along a Vertical Stretching Sheet with Heat Generation. *International Research Journal of Engineering and Technology (IRJET)* e-ISSN: 2395 -0056 Volume: 03 Issue: 02 | Feb-2016 [www.irjet.net](http://www.irjet.net)
- [23]. Khader M. M. and Megahed A. M. (2013), "Numerical solution for boundary layer flow due to a nonlinearly stretching sheet with variable thickness and slip velocity", *Eur. Phys. J. Plus* 128.
- [24]. Lavanya B and Leela Ratnam A. (2014), Dufour and Soret effects on steady MHD free convective flow past a vertical porous plate embedded in a porous medium with chemical reaction, radiation heat generation and viscous dissipation, *Pelagia Research Library, Advances in Applied Science Research*, vol:5(1), pp:127-142.
- [25]. Mahmoud, M.A.A. (2010), "The effects of variable fluid properties on MHD Maxwell fluids over a stretching surface in the presence of heat generation/absorption," *Chem. Eng. Comm.* 198, pp. 131.
- [26]. Mahmoud, M.A.A. (2013), "Heat and mass transfer in stagnation point flow towards a vertical stretching sheet embedded in a porous medium with variable fluid properties and surface slip velocity," *Chem. Eng. Comm.* 200, pp. 543
- [27]. Mahmoud, M.A.A. and Waheed, S.E. (2012), "Variable fluid properties and thermal radiation effects on flow and heat transfer in micropolar fluid film past moving permeable infinite flat plate with slip velocity," *Appl. Math. Mech.-Engl. Ed.* 33, pp. 663
- [28]. Mandal, I.C. and Mukhopadhyay, S. (2013), "Heat transfer analysis for fluid flow over an exponentially stretching porous sheet with surface heat flux in porous medium," *Ain Shams Eng. J.* 4, pp. 103. *Open Science Journal of Mathematics and Application* 2015; 3(2): 26-33
- [29]. Megahed A.M. (2014), "Variable heat flux effect on magnetohydrodynamic flow and heat transfer over an unsteady stretching sheet in the presence of thermal radiation," *Can. J. Phy.* 92, pp. 86.
- [30]. Megahed A.M. (2014), "Numerical solution for variable viscosity and internal heat generation effects on boundary layer flow over an exponentially stretching porous sheet with constant heat flux and thermal radiation," *J. Mech.* 30, pp. 395.
- [31]. Metri Prashant G, Tawade Jagdish, Subhash M, Abel (2016), Thin film flow and heat transfer over an unsteady stretching sheet with thermal radiation, internal heating in presence of external magnetic field. [arXiv:1603.03664v1](https://arxiv.org/abs/1603.03664v1), physics.flu-dyn.
- [32]. Mohammad S., Atif N. and Fatima A. (2015), "Numerical solution of two dimensional stagnation flows of micropolar fluids towards a shrinking sheet by using SOR iterative procedure", *SCITECH Volume 3, Issue 1, RESEARCH ORGANISATION, Journal of Progressive Research in Mathematics (JPRM)* ISSN: 2395-0218
- [33]. Mohammadreza Azimi, Davood Domiri Ganji and Farhad Abbassi (2012), "Study on MHD viscous flow over a stretching sheet using DTM-PADE' technique", *Modern Mechanical Engineering*, 2, 126-129, <http://dx.doi.org/10.4236/mme.24016> Published Online November <http://www.SciRP.org/journal/mme>
- [34]. Muhammad Khairul Anuar Mohamed, Mohd Zuki Salleh, Roslinda Nazar and Anuar Ishak (2013), "Numerical investigation of stagnation point flow over a stretching sheet with convective boundary conditions". *Boundary Value Problems*

2013, <http://www.boundaryvalueproblems.com/content/1/4>

[35]. Mukherjee, B. and Prasad, N. (2014), "Effect of radiation and porosity parameter on hydromagnetic flow due to exponentially stretching sheet in a porous media," *Inter. J. Eng. Sci. Tech.* 6, pp. 58

[36]. Mukhopadhyay S. and Andersson H.I. (2009), "Effect of slip and heat transfer analysis of flow over an unsteady stretching surface", *Heat mass transfer*, vol.45, no.11, pp.1447-1452. doi:10.1007/s11012-009-0516-7.

[37]. Pal, D. (2013), "Hall current and MHD effects on heat transfer over an unsteady stretching permeable surface with thermal radiation," *Comput. Math. Appl.* 66, pp. 1161.

[38]. Prasad K.V., Vajravelu K. and Datti P. S. (2010), The effects of variable fluid properties on the hydromagnetic flow and heat transfer over a non-linearly stretching sheet, *Int. J Ther. Sci.* Vol. 49, 603-610

[39]. Prasanna Kumara C., Ramesh G. K., Chamkha A. J., Gireesha B. J. (2015), "Stagnation-point flow of a viscous fluid towards a stretching surface with variable thickness and thermal radiation". *Int. J. Industrial Mathematics (ISSN 2008-5621)* Vol. 7, No. 1 Article ID IJIM-00582, 9 pages.

[40]. Rao Subba, Prasad V. R., Nagendra N., Murthy K. V. N, Bhaskar Reddy N. and Anwar Beg O. (2015), "Numerical Modeling of Non-Similar Mixed Convection Heat Transfer over a Stretching Surface with Slip Conditions", *World Journal of Mechanics*, 5, 117-128 in *SciRes.*  
<http://www.scirp.org/journal/wjmhttp://dx.doi.org/10.4236/wjm.56013>

[41]. Rashidi M. M and Mohimani Pour S. A (2010), "Analytic approximate solutions for unsteady boundary-layer flow and heat transfer due to a stretching sheet by Homotopy analysis method", *Nonlinear Analysis: Modelling and Control*, 15 ,1, 83-95.

[42]. Rashidi M. M., Rostami B., Freidoonimehr N. and Abbasbandy S. (2014), "Free convective heat and mass transfer for MHD flow over a permeable vertical stretching sheet in the presence of the radiation and buoyancy effects", *Ain Shams Engineering Journal* ,5 ,901-912.

[43]. Sakiadis B.C (1961), "Boundary Layer behavior on continuous solid surface; boundary layer equation for two dimensional and axisymmetric flow" *A.I.Ch.E.J.*, Vol.7, 26-28.

[44]. Sarojamma G., Mahaboobjan Syed and Nagendramma V. (2015), "Influence of hall currents on cross diffusive convection in a MHD boundary layer flow on stretching sheet in porous medium with heat generation", *International Journal of Mathematical Archive-6(3)*, 227-248, [www.ijma.info](http://www.ijma.info) ISSN 2229 – 5046.

[45]. Schlichting H. (1968), "Boundary Layer Theory", McGraw-Hill, New York.

[46]. Sharidan S, Mahmood J. and Pop. I (2008), "Similarity solutions for the unsteady boundary layer flow and Heat Transfer due to a stretching sheet", *Int.J. of Appl. Mechanics and Engineering*, vol.11, No.3, 647-654.

[47]. Sharma P. R., Manishasharma and Yadav R. S. (2015), "Unsteady MHD forced convection flow and mass transfer along a vertical stretching sheet with heat source / sink and variable fluid properties", *international research journal of engineering and technology (irjet)* e-issn: 2395-0056 ,volume: 02 issue: 03 [www.irjet.net](http://www.irjet.net) p-issn: 2395-0072.

[48]. Shit G.C. and Halder R. (2012), "combined effects of thermal radiation and hall current on MHD free-convective flow and mass transfer over a stretching sheet with variable viscosity", *Journal of Applied Fluid Mechanics*, Vol. 5, No. 2, pp. 113-121, [www.jafmonline.net](http://www.jafmonline.net), ISSN 1735-3572, EISSN 1735-3645.

[49]. Soo S.L (1964), "Effect of electrification on the dynamics of a particulate system", *I and EC Fund*, 3:75-80.

[50]. Subhas A.M., and Mahesh N. (2008), "Heat transfer in MHD visco-elastic fluid flow over a stretching sheet with variable thermal conductivity, non-uniform heat source and radiation", *Applied Mathematical Modeling*, 32, 1965-83.

[51]. Tsou F.K., Sparrow E.M. and Glodstein R.J. (1967), "Flow and Heat Transfer in the boundary layer on a continuous moving surface", *Int. J. Heat and Mass transfer*, 10, 219-235.

[52]. Uddin Md. Jashim, Khan W.A., Ahmad Izani Md. Ismail, (2015), Similarity solution of diffusive free convective flow over a moving vertical flat plate with convective boundary condition, *Ain Shams Engineering journal*.

[53]. Vajravelu K. and J. Nayfeh (1992), "Hydromagnetic flow of a dusty fluid over a stretching sheet", *Int.J. of nonlinear Mechanics*, vol.27, No.6, pp.937-945.

[54]. Van Gorder R.A. and Vajravelu (2010), A note on flow geometries and the similarity solutions of the boundary layer equations for a nonlinearly stretching sheet, *Arch. Appl. Mech.* Vol. 80 ,1329–1332.

**Nomenclature:**

x, y - Cartesian coordinates	$P_r$ - Prandtl number
$\eta$ - Similarity variable	$G_r$ - Grashof number
u - Velocity component of fluid along x-axis	$F_r$ - Froude number
v - Velocity component of fluid along y-axis	$E_c$ - Eckert number
$u_p$ - Velocity component of the particle along x-axis	$\omega$ - Density ratio

$v_p$ -Velocity component of the particle along y-axis	$\phi$ -Volume fraction
$U_w(x)$ -Stretching sheet velocity	$c$ -Stretching rate
$M$ - Electrification parameter	$l$ -Characteristic length
$E$ -Electric field of force	$c_p$ - Specific heat of fluid
$m$ -Mass of particle	$c_s$ -Specific heat of particles
$e$ -Charge of particle	$k_s$ -Thermal conductivity of particle
$T$ -Temperature of fluid phase.	$k$ -Thermal conductivity of fluid
$T_p$ -Temperature of particle phase.	$A$ -Unsteady parameter
$T_w$ -Wall temperature	$a$ - Constant
$T_\infty$ -Temperature at large distance from the wall.	$\beta$ -Fluid particle interaction parameter
$A^*$ and $B^*$ - Non dimensional heat generation/absorption parameter for fluid phase	$\tau_T$ -Thermal relaxation time i.e. the time required by the dust particle to adjust its temperature relative to the fluid.
$A_p^*$ and $B_p^*$ -Non dimensional heat generation/absorption parameter for particle phase	$\tau_p$ -Velocity relaxation time i.e. the time required by the dust particle to adjust its velocity relative to the fluid.
$\theta$ - Non-dimensional fluid phase temperature	$\tau$ -Relaxation time of particle phase
$\theta_p$ - Non-dimensional dust phase temperature	$\mu$ -Dynamic viscosity of fluid
$Ra$ -Radiation parameter	$\nu$ -Kinematic viscosity of fluid
$q_{rp}$ -Radiate heat flux for particle phase	$\gamma$ -Ratio of specific heat
$q_r$ -Radiate heat flux for fluid phase	$\epsilon$ - Diffusion parameter
$\beta^*$ -volumetric coefficient of thermal expansion	$\rho$ -Density of the fluid phase
$k^*$ -Mean absorption coefficient.	$\rho_s$ - Material density
$\sigma^*$ - Stefan-Boltzman constant	$\rho_p$ -Density of the particle phase

“TABLE-1”: Comparison results for the wall temperature gradient  $-\theta'(0)$  in the case of  $\beta, A^*, B^*, A_p^*, B_p^*, Ra, Gr, Ec, A, M, \phi = 0.0$

$P_r$	Chen C.H. [8]	Grubka L.J. et.al.[19]	Subhas A.et.al.[50]	Mukhopadhaya S.et.al.[36]	Ishak et.al. A [21]	Gireesha B.J.et.al.[16]	Present Study $-\theta'(0)$
0.72	1.0885	1.0885	1.0885	1.0885	-	1.0885	1.088635
1.0	1.3333	1.3333	1.3333	1.3333	1.3333	1.3333	1.333927
3.0	2.5097	-	-	2.5097	2.5097	2.5097	2.509564

“TABLE-2”: Initial values of wall velocity gradient  $-f''(0)$  and temperature gradient  $-\theta'(0)$

$\phi$	$\beta$	$\epsilon$	$A$	$A^*$	$B^*$	$A_p^*$	$B_p^*$	$M$	$Ec$	$P_r$	$Gr$	$Ra$	$-f''(0)$	$-\theta'(0)$
0	0	0	0	0	0	0	0	0	0	0.72	0	0	1.001396	1.082315
0.01	0.01	5.0	0.1	0.1	0.1	0.1	0.1	0.1	1.0	0.71	0.01	1.0	1.011790	0.553447
0.1													1.010030	0.553648
0.3													1.004963	0.556359
0.5													0.995560	0.563478
0.01	0.01	5.0	0.1	0.1	0.1	0.1	0.1	0.1	1.0	0.71	0.01	1.0	1.011790	0.553447
		0.02											1.010760	0.554952
		0.03											1.012920	0.549767
0.01	0.01	5.0	0.1	0.1	0.1	0.1	0.1	0.1	1.0	0.71	0.01	1.0	1.011790	0.553447

		5.5											1.011538	0.551914
		6.0											1.011449	0.551094
0.01	0.01	5.0	0.1	0.1	0.1	0.1	0.1	0.1	1.0	0.71	0.01	1.0	1.011790	0.553447
			0.2										1.048937	0.597137
			0.3										1.084461	0.640866
				-0.5									1.012777	0.755196
				-0.1									1.012232	0.619318
				0.0									1.012135	0.585140
0.01	0.01	5.0	0.1	0.1	0.1	0.1	0.1	0.1	1.0	0.71	0.01	1.0	1.011790	0.553447
				0.5									1.011339	0.414973
					-0.5								1.013463	0.783452
					-0.1								1.012409	0.641113
					0.0								1.012396	0.595400
0.01	0.01	5.0	0.1	0.1	0.1	0.1	0.1	0.1	1.0	0.71	0.01	1.0	1.011790	0.553447
					0.5								1.010519	0.308891
						-0.5							1.011781	0.553444
						-0.1							1.011785	0.553445
						0.0							1.011789	0.553446
0.01	0.01	5.0	0.1	0.1	0.1	0.1	0.1	0.1	1.0	0.71	0.01	1.0	1.011790	0.553447
						0.5							1.011791	0.553448
							-0.5						1.011785	0.553411
							-0.1						1.011788	0.553438
							0.0						1.011789	0.553443
0.01	0.01	5.0	0.1	0.1	0.1	0.1	0.1	0.1	1.0	0.71	0.01	1.0	1.011790	0.553447
							0.5						1.011792	0.553461
								0.0					1.029781	0.536832
								0.05					1.020120	0.544887
								0.08					1.013691	0.549911
0.01	0.01	5.0	0.1	0.1	0.1	0.1	0.1	0.1	1.0	0.71	0.01	1.0	1.011790	0.553447
									0.0				1.012108	0.687354
									1.0				1.011790	0.553447
									2.0				1.011686	0.414141
									3.0				1.011387	0.277564
										0.1			1.009487	0.155226
										0.5			1.011763	0.434192
0.01	0.01	5.0	0.1	0.1	0.1	0.1	0.1	0.1	1.0	0.71	0.01	1.0	1.011790	0.553447
										1.0			1.012418	0.689271
										2.0			1.013572	1.041177
										3.0			1.014353	1.298455
											0.01	1.0	1.011790	0.553447
											0.03		0.999476	0.556873
											0.05		0.999474	0.556876
0.01	0.01	5.0	0.1	0.1	0.1	0.1	0.1	0.1	1.0	0.71	0.01	1.0	1.011790	0.553447
												2.0	1.011573	0.449928
												3.0	1.011086	0.397243

**Aswin Kumar Rauta** was born in Khallingi of district Ganjam, Odisha, India. He obtained the M.Sc. and M.Phil. Degree in Mathematics from Berhampur University, Berhampur, Odisha, India in 2003 and 2007 respectively. He got Ph.D degree in Mathematics on the research topic 'Modeling of two phase flow' from Berhampur University, Odisha, India in 2016. He has qualified NET in 2009 conducted by CSIR-UGC, government of India and is continuing his research work since 2009 and works till today. His field of interest covers the areas of application of boundary layer, heat/mass transfer and dusty fluid flows. He joined as a lecturer in Mathematics in the Department of Mathematics, S.K.C.G.College, Paralakhemundi, Odisha, India in 2011 and is continuing his job.

**Dr.Saroj Kumar Mishra** was born in Narsinghpur of Cuttuckdistrict,Odisha,India.He received his M.Sc. degree in Mathematics in 1976 and Ph.D in Mathematics in 1982 on the research topic “Dynamics of two phase flow” from IIT Kharagpur, India . Currently he is working as Adjunct Professor of Mathematics at Centre for Fluid Dynamics Research, CUTM, Paralakhemundi, Odisha, India. He has authored and coauthored 50 research papers published in national and international journal of repute. His research interest includes the area of fluid dynamics, dynamics of dusty fluid particularly, in boundary layer flows, heat transfer, MHD, FHD and flow through porous media. His research interest also covers the nano fluid problems, existence and stability of problems.